athermal associated solution model (Tables VIII and IX).

In the low concentration region herein examined, chemical equilibrium constants are much lower than those calculated from pure alcohol properties (*14*) (Table XI). More recent information (*15*) about equilibrium constants does not alter significantly the differences. It must be pointed out, however, that these constants are extrapolated from vapor pressure data at temperatures higher than those considered in this work.

Again, as in the case of cyclohexane as the solvent (*1*) the differences may be attributed to an influence of the concentration in the region of high dilution, in spite of the aromaticity of thiophene, which should be considered in some way in the theory of associated solutions.

Glossary

a_1	activity of the solvent
A, B	constants (see eq 3)
A_0, A_1, A_2	constants (see eq 6)
A_{12}, A_{21}	van Laar parameters
c_p	heat capacity
K, K_A, K_1, K_2	chemical equilibrium constants
N	number of experimental data points
R	gas constant
S	extent of supercooling
T	absolute temperature
T_0	melting point of the solvent
T_s	lowest temperature of supercooled solution
x_1, x_2	mole fractions of solvent and solute
z	mole fraction ratio x_2/x_1
β	parameter in ideal associated solution model
γ_1, γ_2	activity coefficients of solvent and solute
Δ	difference
ϵ	see eq 13 and 15
η	see eq 12 and 14
θ	freezing point depression calculated from a model
$\hat{\theta}$	corrected experimental freezing point depression
θ_m	measured experimental freezing point depression
λ_{ij}, Λ_{ij}	Wilson equation parameters
λ_1	heat of fusion of solvent
σ	standard deviation
ϕ	osmotic coefficient
χ	Scatchard–Hildebrand type parameter
ψ_θ, ψ_γ	objective functions

Registry No. Thiophene, 110-02-1; 1-butanol, 71-36-3; 2-butanol, 78-92-2; isobutyl alcohol, 78-83-1; *tert*-butyl alcohol, 75-65-0.

Literature Cited

(1) Aguirre-Ode, F. *J. Chem. Eng. Data* **1987**, *32*, 434.
(2) Timmermans, J. *Physico-Chemical Constants of Pure Organic Compounds*; Elsevier: New York, 1950.
(3) Wilhoit, R. C., Zwolinski, B. J., *J. Phys. Chem. Ref. Data* **1973**, *2*, Suppl. No. 1.
(4) Gillespie, R. J., Hughes, E. D., Ingold, C. K. *J. Chem. Soc.* **1950**, 2472.
(5) Prigogine, I., Defay, R. *Chemical Thermodynamics*; Wiley: New York, 1962; p 359.
(6) Waddington, G., Knowlton, J. *J. Am. Chem. Soc.* **1949**, *71*, 798.
(7) Figuiere, P., Szwarc, H., Masaharu, O., Suga, H. *J. Chem. Thermodyn.* **1985**, *17*, 949.
(8) Prigogine, I., Defay, R. *Chemical Thermodynamics*; Wiley: New York, 1962; p 324.
(9) van Laar, J. J. *Z. Phys. Chem.* **1910**, *72*, 723.
(10) Wilson, G. M. *J. Am. Chem. Soc.* **1984**, *86*, 127.
(11) Aguirre-Ode, F. *Scientia* **1977**, *42*(149), 25.
(12) Aguirre-Ode, F. *Scientia* **1979**, *44*(152), 19.
(13) Aguirre-Ode, F. *Fluid Phase Equilib.* **1986**, *30*, 315.
(14) Nath, A., Bender, E. *Fluid Phase Equilib.* **1981**, *7*, 275.
(15) Hofman, T., Nagata, I. *Fluid Phase Equilib.* **1986**, *25*, 113.

Received for review July 22, 1987. Revised February 16, 1988. Accepted March 9, 1988. Financial support by FONDECYT (Chile) is duly acknowledged.

Equilibrium-Phase Properties of the Neopentane–Carbon Dioxide Binary System

Ah-Dong Leu and Donald B. Robinson*

Department of Chemical Engineering, University of Alberta, Edmonton, Alberta, Canada T6G 2G6

Vapor and liquid equilibrium-phase compositions were determined for the neopentane–carbon dioxide system at 40, 65, 90, 120, and 150 °C from the vapor pressure of neopentane to pressures in the critical region. The equilibrium ratios for each component were calculated at each temperature from the phase composition data. The critical pressure corresponding to each of the experimental temperatures was measured and the critical locus for the binary was constructed.

Introduction

Carbon dioxide is a very important industrial raw material and its uses range from the enhanced recovery of conventional and heavy oil to supercritical extraction processes in the food industry. Because of the current interest in the behavior of gas and liquid systems containing carbon dioxide, users of basic thermodynamic data are becoming increasingly sensitive to the reliability of existing data, and they show considerable interest in expanding the pressure and temperature ranges and the number of systems for which data are available.

A literature survey pertaining to the phase behavior of carbon dioxide–paraffin hydrocarbon binaries has revealed that the work of Schwartz et al. (*1*) and Stead et al. (*2*) represents the only data on the neopentane–carbon dioxide system. In their studies, the highest temperature was 27 °C. Accordingly, it was decided to carry out an experimental study of this system in the temperature range from 40 °C to near the critical temperature of neopentane. Data in this region are useful for developing improved generalized equation of state parameters for neopentane–carbon dioxide mixtures.

In addition to the phase composition measurements, critical temperatures and corresponding critical pressures were ob-

---

* Author to whom all correspondence should be addressed.

0021-9568/88/1733-0313$01.50/0

tained from which the critical locus for this binary system could be constructed.

Equipment and Experimental Method

The experiments were carried out in a variable volume vapor–liquid equilibrium cell consisting of a transparent sapphire cylinder mounted between two steel headers. The design and operation of this equipment has been described in detail by Robinson et al. (*3*) and by Huang et al. (*4*).

Prior to commencing an experimental run, the equipment was thoroughly cleaned and evacuated. Neopentane was then added to the cell, followed by carbon dioxide. The contents of the cell were mixed by rocking the entire cell assembly, and during this process the cell was brought to the desired temperature and pressure. When equilibrium had been established, the rocking motion was stopped and the sampling process commenced.

The gas phase was sampled by continuously drawing off a vapor stream through the sampling valve under isobaric isothermal conditions. The sample was mixed with a stream of helium and circulated through the chromatographic switching valve. Samples were taken for analysis at periodic intervals. After the vapor phase had been analyzed, the remainder of the vapor phase plus a small interface portion were removed. The liquid phase was then sampled and analyzed by using a similar procedure.

At the completion of each pressure point, a new set of conditions was established by adjusting pressure and/or adding more material and the equilibration and sampling sequence was repeated.

The critical point was obtained at isothermal conditions by adjusting the pressure and/or adding more material. As equilibrium was approached in the critical region, minor isothermal adjustments in the pressure were made to observe changes along the phase boundary and to note the critical opalescence. When the critical pressure had been determined, the pressure was increased well into the single-phase region so that the system could be sampled and analyzed to obtain the composition at the critical point.

Temperatures were measured with iron–constantan thermocouples that had been calibrated against a platinum resistance thermometer. Each temperature was read out on a digital voltmeter (HP-3455A). Temperatures are believed known to within ±0.1 °C.

Pressures were measured with a 0–1500 psia strain gauge pressure transducer (Bell & Howell 4-356-0003) calibrated with a dead weight gauge. Each pressure was read out on a digital voltmeter (HP-3455A). The pressure is believed known to within ±0.15% of the full scale.

The phase compositions were determined with a Hewlett-Packard Model 5750B gas chromatograph coupled with a HP-3353 data acquisition system. A thermal conductivity detector on isothermal mode was used. Calibration was made for each component using a gravimetric method. Relative response factors were obtained from peak areas vs sample size. The column was made from 3.18 mm diameter stainless steel tubing and was 2.44 m long. It was packed with Porapak QS and maintained at 140 °C.

The response factor for converting area fraction to mole fraction was 1.7664 for neopentane compared to 1.0000 for carbon dioxide. At least eight samples of each phase were taken for analysis. The reported compositions are the result of averaging at least six determinations. The precision of the analyses was generally within 2% relative standard deviation.

In determining the physical properties in the critical region, the experimental temperature was considered to be the critical temperature, and the corresponding critical pressure was determined by averaging the two values obtained in the immediate vicinity of but on either side of the critical point from isothermal compression and expansion observations. The associated composition was determined as described above.

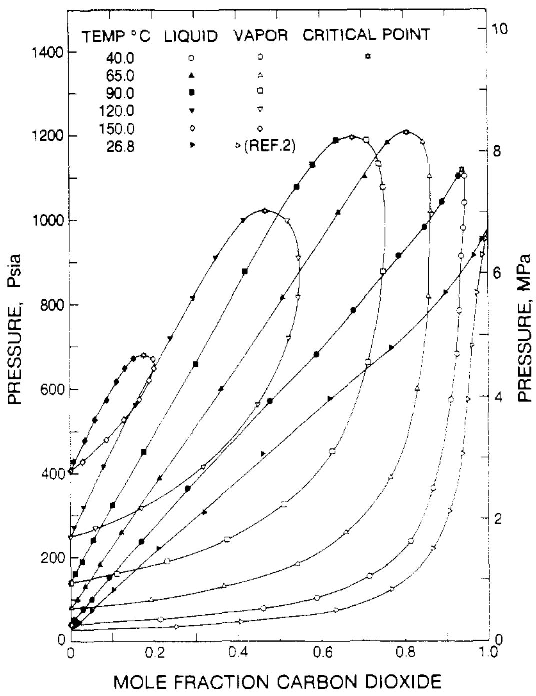

Figure 1. Pressure–equilibrium-phase-composition diagram for the neopentane–carbon dioxide binary system.

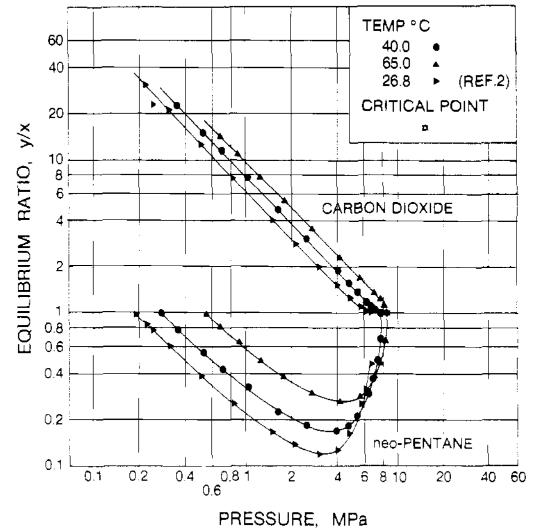

Figure 2. Equilibrium ratios for neopentane and carbon dioxide in the neopentane–carbon dioxide binary system at 40.0, 65.0, and 90.0 °C.

The Research Grade 2,2-dimethylpropane (neopentane) had a purity of 99.86 mol % and was obtained from Matheson Gas Products Canada, Inc. A chromatogram was run on this compound but no detectable impurities were found. The neopentane was degassed in the equilibrium cell before the introduction of carbon dioxide. Industrial grade carbon dioxide containing 99.9+ mol % purity was obtained from the Linde Division of Union Carbide. Both materials were used without further purification.

Results and Discussion

The experimental measurements of the equilibrium phase compositions for the neopentane–carbon dioxide system are given in Table I. The vapor- and liquid-phase envelopes for the system are shown in Figure 1 for five isotherms at 40, 65,

Table I. Equilibrium-Phase Properties of the Neopentane–Carbon Dioxide System

pressure		composition[a]		equilib const	
psia	MPa	x	y	K_{CO_2}	$K_{neo\text{-}C_5}$
		T = 40.0 °C			
41	0.283	0	0		1.000
52	0.358	0.2140	0.0093	23.0	0.793
77	0.531	0.4612	0.0306	15.06	0.556
102	0.703	0.5884	0.0509	11.56	0.434
152	1.05	0.7140	0.0924	7.73	0.315
236	1.63	0.8145	0.1703	4.78	0.224
364	2.51	0.8672	0.2804	3.09	0.184
571	3.94	0.9115	0.4767	1.91	0.169
680	4.69	0.9259	0.5903	1.57	0.181
784	5.41	0.9304	0.6777	1.37	0.216
912	6.29	0.9373	0.7874	1.19	0.295
979	6.75	0.9427	0.8471	1.11	0.375
1039	7.16	0.9465	0.8907	1.06	0.489
1103	7.61	0.9459	0.9297	1.02	0.769
1116	7.70	0.9395	0.9395	1.00	1.00
		T = 65.0 °C			
79	0.545	0	0		1.00
98	0.676	0.1929	0.0136	14.2	0.82
129	0.889	0.3696	0.0335	11.0	0.65
182	1.26	0.5442	0.0718	7.58	0.49
257	1.77	0.6595	0.1203	5.48	0.39
388	2.69	0.7654	0.2127	3.60	0.30
598	4.12	0.8308	0.3607	2.30	0.26
815	5.62	0.8590	0.5065	1.70	0.29
1017	7.01	0.8639	0.6435	1.34	0.38
1101	7.59	0.8610	0.7046	1.22	0.47
1184	8.16	0.8463	0.7632	1.11	0.65
1205	8.31	0.8075	0.8075	1.00	1.00
		T = 90.0 °C			
139	0.958	0	0		1.00
160	1.10	0.1117	0.0110	10.2	0.90
190	1.31	0.2331	0.0273	8.53	0.79
241	1.66	0.3751	0.0550	6.82	0.66
324	2.23	0.5108	0.1013	5.05	0.54
450	3.10	0.6259	0.1740	3.60	0.45
661	4.56	0.7125	0.3007	2.37	0.41
875	6.03	0.7505	0.4203	1.79	0.43
1076	7.42	0.7500	0.5425	1.38	0.55
1131	7.80	0.7400	0.5824	1.27	0.62
1186	8.18	0.7127	0.6370	1.12	0.79
1193	8.22	0.6776	0.6776	1.00	1.00
		T = 120.0 °C			
246	1.70	0	0		1.00
267	1.84	0.0605	0.0097	6.2	0.95
317	2.19	0.1700	0.0330	5.15	0.86
415	2.86	0.3170	0.0810	3.91	0.74
562	3.88	0.4502	0.1567	2.87	0.65
719	4.96	0.5246	0.2395	2.19	0.63
816	5.63	0.5479	0.2952	1.86	0.64
909	6.27	0.5491	0.3508	1.56	0.69
998	6.88	0.5214	0.4179	1.25	0.82
1019	7.03	0.4690	0.4690	1.00	1.00
		T = 150.0 °C			
407	2.81	0	0		1.00
428	2.95	0.0288	0.0098	2.9	0.98
479	3.30	0.0864	0.0344	2.51	0.95
527	3.63	0.1289	0.0596	2.16	0.92
574	3.96	0.1650	0.0873	1.89	0.92
618	4.26	0.1885	0.1112	1.70	0.91
648	4.47	0.2014	0.1313	1.53	0.92
671	4.63	0.1994	0.1512	1.32	0.94
678	4.68	0.1776	0.1776	1.00	1.00

[a] Mole fraction carbon dioxide.

90, 120, and 150 °C. The calculated equilibrium ratios for each component at each of the five temperatures are also given in Table I and are shown graphically in Figures 2 and 3.

The measured critical temperatures and corresponding pressures for this binary system are presented in Table II and the critical locus is shown graphically in Figure 4.

A comparison of the critical locus for this system with that for the *n*-pentane–carbon dioxide system (*5*) shows that the cricondenbar for the neopentane binary is about 1.550 MPa lower than that for the *n*-pentane binary.

The experimental data on the behavior of the neopentane–carbon dioxide binary system will be useful for evaluating the optimum binary interaction parameters in equation of state modeling of systems containing these components.

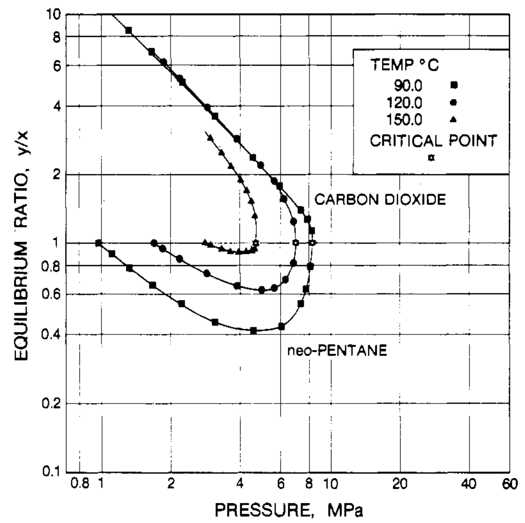

Figure 3. Equilibrium ratios for neopentane and carbon dioxide in the neopentane–carbon dioxide binary system at 90.0, 120.0, and 150.0 °C.

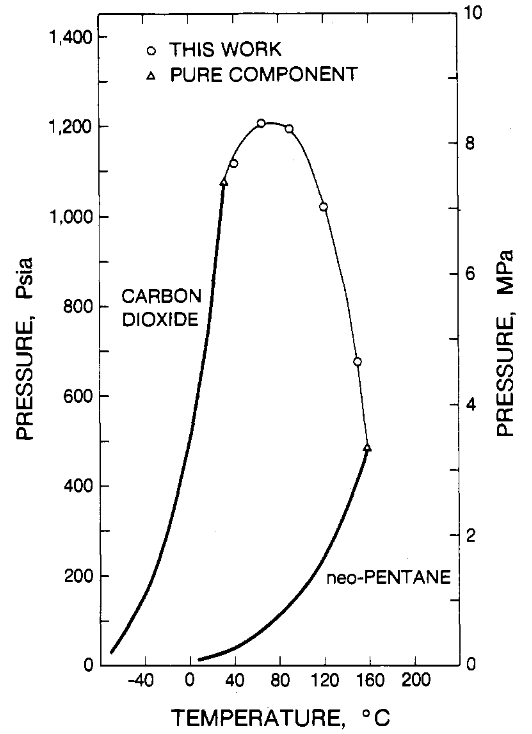

Figure 4. Critical locus for the neopentane–carbon dioxide binary system.

Table II. Critical Temperatures and Pressures for the Binary System Neopentane–Carbon Dioxide

crit temp, °C	crit press., MPa	crit temp, °C	crit press., MPa
40.0	3.70	120.0	7.03
65.0	8.31	150.0	4.68
90.0	8.22		

Glossary

K	equilibrium ratio y/x
K_{CO_2}	equilibrium ratio for carbon dioxide
$K_{neo\text{-}C_5}$	equilibrium ratio for neopentane
P	pressure
T	temperature
x	mole fraction of component in liquid phase
y	mole fraction of component in vapor phase

Registry No. CO_2, 124-38-9; neopentane, 463-82-1.

Literature Cited

(1) Schwartz, A. S.; Donnelly, H. G. *Chem. Eng. Prog. Symp. Ser.* **1968**, *64*(88), 44–56.
(2) Stead, K.; Williams, H. M. *J. Chem. Thermodyn.* **1980**, *12*, 265–275.
(3) Robinson, D. B.; Huang, S.-S.; Leu, A.-D.; Ng, H.-J. Research Report RR-57, Gas Processors Association, February, 1982.
(4) Huang, S.-S.; Leu, A.-D.; Ng, H.-J.; Robinson, D. B. *Fluid Phase Equilib.* **1985**, *19*, 21–32.
(5) Leu, A.-D.; Robinson, D. B. *J. Chem. Data* **1987**, *32*, 447–450.

Received for review July 15, 1987. Accepted March 6, 1988. The financial support of the Natural Sciences and Engineering Research Council for this work is acknowledged and appreciated.

Vapor–Liquid Equilibria for Binary Mixtures of Butyl Ether with 2-Furaldehyde and with 2-, 3-, and 4-Heptanone

Huey S. Wu and Stanley I. Sandler*

Department of Chemical Engineering, University of Delaware, Newark, Delaware 19716

Isomeric effect on group-contribution liquid-activity models has been investigated by accurate measurement of vapor–liquid equilibria of butyl ether separately with 2-, 3-, and 4-heptanone, each on two isotherms. We also report data for butyl ether and 2-furaldehyde on two isotherms. The data reported satisfy thermodynamic consistency tests. The results of our measurements are correlated with five thermodynamic models by using the maximum likelihood parameter estimation method. A previously unavailable pair of UNIFAC interaction parameters for the furfural group with an ether group are also estimated from our data.

Introduction

Highly accurate vapor–liquid equilibria (VLE) are important to the design of separation processes and in the testing and further development of thermodynamic models. Recent group-contribution activity-coefficient models, e.g., UNIFAC (*1*, *2*) or TOM (*3*, *4*), are useful predictive models, but they do have some limitations. For example, the UNIFAC model cannot differentiate between some isomers, while isomeric mixtures do occur quite often in chemical processing. The TOM Project differentiates between isomers (*5*), but its further development will need additional accurate measurements, such as the data reported here. In this study the VLE of butyl ether separately with three isomers of heptanone were measured, and the experimental data compared with the predictions of the UNIFAC model. We have also measured the VLE of butyl ether with 2-furaldehyde (or furfural) and used these data to estimate the previously unavailable UNIFAC interaction parameters for the furfural group with an ether group.

In this study we report the results of our measurements of the pure component vapor pressures of butyl ether, and of 2-, 3-, and 4-heptanone, and the binary VLE of butyl ether separately with 2-heptanone at 363.15 and 393.22 K, with 3-heptanone and 4-heptanone at 363.15 and 393.15 K, and with furfural at 368.15 and 388.15 K. Our experimental data satisfy the thermodynamic consistency tests. Data reduction was carried out to determine the excess molar Gibbs free energies, G^E, for each isotherm, and to calculate molar heat of mixing using the Gibbs–Helmholtz relation.

Experiments

The experimental equipment and operating procedure have been described previously (*5*). Due to the rapid oxidation and autooxidation of furfural, the special methods of handling furfural previously reported (*6*) were used. The VLE measurements for both pure components and mixtures were made with a Stage-Muller dynamic still. The temperature was measured with a platinum resistance thermometer (Rosemount Model 162N) accurate to 0.02 K with a resolution of 0.001 K. Pressure was measured with an accuracy of 0.02 kPa by using a Wallace-Tiernan Model FA-187 precision mercury manometer. Vapor and liquid equilibrium samples were analyzed by a Hewlett-Packard Model 5730 gas chromatograph with a Model 3390 integrator, after calibration with gravimetrically prepared samples. The compositions determined are accurate to better than 0.005 in mole fraction.

Since the purity of chemicals is essential for accurate VLE measurements, we checked the purity of each chemical first by measuring its area fraction by gas chromatography, and then by comparing its pure component vapor pressure measured in the Stage-Muller still with data reported in the literature. In this study all chemicals used were from the Aldrich Chemical Co. Butyl ether was Gold Label quality of 99.9% purity by GC analysis as received. However, butyl ether is highly hygroscopic, and we found that it was rapidly contaminated by moisture. Therefore, when measuring the butyl ether vapor pressure, we constantly checked the water content of the solution in our still by gas chromatography. When the water content was above 0.1%, the still contents were replaced with fresh anhydrous butyl ether. Our measured butyl ether vapor pressure data are shown in Table I, and compared, in Table II, with predictions using Antoine constants reported in literature (*7*). We believe our vapor pressure data to be correct and that the higher vapor pressures reported previously in the literature are likely to result from contamination by water. The Antoine constants for furfural were found to be the same as in our previous report (*6*). The heptanones did not satisfy our purity tests as received and were purified to 99.9% by using a 13-stage Oldershaw distillation column at low pressure under a nitrogen blanket. The vapor pressures of three purified hep-

0021-9568/88/1733-0316$01.50/0